Drought-induced vegetation stress in southwestern North America

Drought-induced vegetation stress in southwestern North America

Xiaoyang Zhang[1,5]**, Mitchell Goldberg**[2]**, Dan Tarpley**[2]**,
Mark A Friedl**[3]**, Jeffrey Morisette**[4]**, Felix Kogan**[2] **and Yunyue Yu**[2]

[1] Earth Resources Technology Incorporated at NOAA/NESDIS/STAR, 5200 Auth Road,
Camp Springs, MD 20746, USA

[2] NOAA/NESDIS/STAR, 5200 Auth Road, Camp Springs, MD 20746, USA

[3] Department of Geography and Environment, Boston University, 675 Commonwealth
Avenue, Boston, MA 02215, USA

[4] Invasive Species Science Branch, US Geological Survey, Fort Collins Science Center,
2150 Centre Avenue, Building C, Fort Collins, CO 80526-8118, USA

E-mail: xiaoyang.zhang@noaa.gov

Abstract
Trends towards earlier greenup and increased average greenness have been widely reported in
both humid and dry ecosystems. By analyzing NOAA (National Oceanic and Atmospheric
Administration) AVHRR (Advanced Very High Resolution Radiometer) data from 1982 to
2007, we report complex trends in both the growing season amplitude and seasonally integrated
vegetation greenness in southwestern North America and further highlight regions consistently
experiencing drought stress. In particular, greenness measurements from 1982 to 2007 show an
increasing trend in grasslands but a decreasing trend in shrublands. However, vegetation
greenness in this period has experienced a strong cycle, increasing from 1982 to 1993 but
decreasing from 1993 to 2007. The significant decrease during the last decade has reduced
vegetation greenness by 6% in shrublands and 13% in grasslands (16% and 21%, respectively,
in the severe drought years). The greenness cycle correlates to both annual precipitation and dry
season length derived from NOAA North America Regional Reanalysis data. If drought events
continue as predicted by climate models, they will exacerbate ecosystem degradation and
reduce carbon uptake.

Keywords: interannual vegetation greenness, daily precipitation, dry season length, climate
change, long time series, AVHRR NDVI, complex trends

1. Introduction

Climate change has resulted in substantial surface warming in the past three decades globally (Hansen *et al* 2006) and by as much as 0.3–0.4 °C/decade from the 1970s to 2006 in the western United States (van Mantgem *et al* 2009). This has raised concerns about the impact of temperature changes on terrestrial ecosystem productivity (Nemani *et al* 2003) and a gradual shift of vegetation seasonality (Myneni *et al* 1997, Zhang *et al* 2007). However, warming-induced changes in

precipitation have also caused complex and abrupt terrestrial ecosystem responses (Martiny *et al* 2005, Lotsch *et al* 2005, Peñuelas *et al* 2004). With dryland (arid and semiarid) ecosystems occupying over 5.06×10^9 ha (41%) of land globally (of which, 5.47×10^8 ha are distributed throughout North America and 3.90×10^8 ha throughout the United States), the impact of drought stress on these ecosystems ranks among the most significant environmental challenges today (MEA 2005, Reynolds *et al* 2007).

Vegetation phenology in dryland ecosystems is significantly influenced by water availability. It is therefore sensitive to global climate changes that modify the seasonality of

---

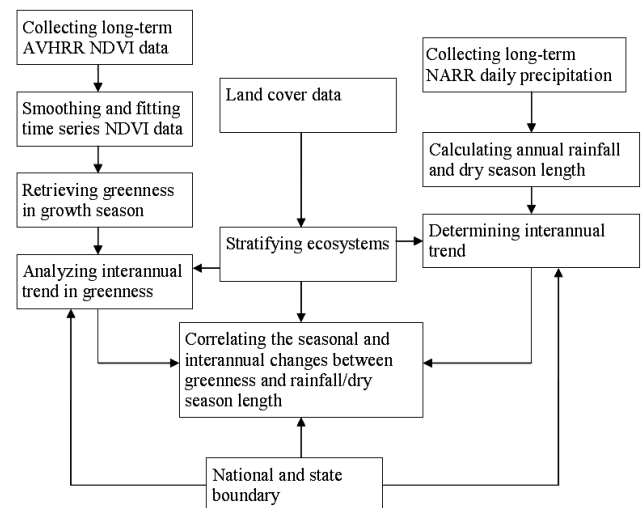[5] Author to whom any correspondence should be addressed.

Figure 1. Ecosystem types stratified from MODIS 1 km land cover types in southwestern North America (95°W–125°W and 20°N–50°N). The states are denoted as WA—Washington, OR—Oregon, CA—California, NV—Nevada, AZ—Arizona, ID—Idaho, UT—Utah, NM—New Mexico, TX—Texas, OK—Oklahoma, KS—Kansan, CO—Colorado, WY—Wyoming, NE—Nebraska, SD—South Dakota, MT—Montana, ND—North Dakota. The gray line indicates the rough location of the Rocky Mountains. Note that shrublands here consist of open shrublands, closed shrublands, and barren-sparsely-vegetated lands.

Figure 2. Flowchart of qualifying interannual variation in vegetation greenness and precipitation.

rainfall, the occurrence of extreme weather events, and the frequency and persistence of rainfall deficits or excesses (e.g., Tyson 1991, Fauchereau *et al* 2003). As a result, precipitation controls the emergence of green leaves, vegetation growing season duration, vegetation primary production, and the geographic distribution of water sensitive biomes (Reich 1995, Justiniano and Fredericksen 2000, Kramer *et al* 2000, Spano *et al* 1999, Cook and Heerdegen 2001, Zhang *et al* 2005).

On a regional scale, the impacts of rainfall on large scale ecosystem dynamics have been investigated using satellite and precipitation data. Previous studies suggest that normalized difference vegetation index (NDVI) data calculated from the Advanced Very High Resolution Radiometer (AVHRR) are strongly correlated to the amount of monthly rainfall (Fuller and Prince 1996, Schmidt and Karnieli 2000), seasonally-aggregated rainfall (Srivastava *et al* 1997), and annually-integrated precipitation (Tucker and Nicholson 1999). More recently, analysis of both monthly global precipitation and AVHRR NDVI has shown the dependence of terrestrial ecosystems on precipitation regimes (Lotsch *et al* 2003). Further, by coupling daily vegetation index data derived from MODIS (Moderate-Resolution Imaging Spectroradiometer) and daily rainfall data retrieved from TRMM (Tropical Rainfall Measuring Mission) Zhang *et al* (2005) characterized how rainy season dynamics control the start and end of vegetation growth in arid and semi-arid African ecosystems (Zhang *et al* 2005).

Interannual trends in vegetation greenness derived from AVHRR data during the 1980s and 1990s have been widely

reported in many global ecosystems. In particular, increasing monthly average NDVI during specific parts of the growing season have been found in both humid climate regions (Myneni *et al* 1997, Zhou *et al* 2001) and arid environments (Olsson *et al* 2005, Piao *et al* 2006). However, little effort has focused on examining interannual variation in cumulative greenness and the amplitude of growing season greenness, which is an important proxy of ecosystem net primary production and carbon sequestration (Posse and Cingolani 2004, Goward *et al* 1985, Tucker *et al* 1986). This study investigates spatio-temporal patterns in satellite-derived greenness growth in response to interannual variations in rainfall and quantifies the magnitude of greenness reduction during a severe drought stress across southwestern North America (95°W–125°W and 20°N–50°N, figure 1). To examine this, AVHRR NDVI data from 1982 to 2007 are employed to calculate vegetation greenness during the growing season after explicitly identifying vegetation phenological transition dates (greenup onset and dormancy onset). Further, complex patterns in greenness associated with dynamics in rainfall and dry season length, calculated from the NCEP (National Centers for Environmental Prediction) North America Regional Reanalysis (NARR) data from 1981 to 2007, are also explored.

2. Methods

The focus of this research is to examine interannual trends and responses in satellite-derived vegetation greenness to climate changes in southwestern North America. To this end, we analyze long-term AVHRR NDVI data and NARR daily precipitation data following the general methodology summarized in figure 2.

2.1. AVHRR data and vegetation greenness detections

The NOAA (National Oceanic and Atmospheric Administration) NESDIS (National Environmental Satellite, Data, and

Information Service) has developed a weekly global vegetation index (GVIx) product with a spatial resolution of 0.036° (about 4 km at the equator) spanning the period from November 1981 to the present (Kogan *et al* 2003). GVIx is produced by reading geo-location (latitude and longitude), sensor, solar and relative azimuth angle, reflectance, brightness temperature, cloud mask, and calibration information from CLAVR-x (Clouds from AVHRR Extended system), which processes AVHRR global area coverage (GAC) level 1B data (Donahue *et al* 2005). The GVIx product is derived from daytime overpasses of NOAA-7, NOAA-9, NOAA-11, NOAA-14, and NOAA-16. The impact of orbital and AVHRR sensor drift on the red and near infrared bands are calibrated using updated post-launch coefficients (Rao and Chen 1995, Gutman *et al* 1995). Weekly NDVI composites are generated from daily arrays using maximum value composites (MVCs) after the observations with large view angles are removed. The NDVI provides a measure of vegetation greenness sensitive to the presence, density, productivity, and condition of green vegetation (Tucker 1979).

Greenness dynamics during the growing season are characterized using NDVI time series and phenological transition dates. First, pixels with cloud or snow contamination are identified using information in the quality assurance flag of the GVIx product. These contaminated data are replaced using a moving window average based on the four nearest neighbors with valid data (Zhang *et al* 2006). Second, contaminated values are further minimized using the representative background NDVI value at each pixel, which represents the minimum NDVI of soil and vegetation in an annual time series (Zhang *et al* 2007). Third, piecewise logistic functions (Zhang *et al* 2003) are used to fit the annual time series of NDVI data from January to December and from July to the following June. This approach ensures that the growing seasons in both summer and winter are captured. Fourth, the fitted functions are applied to detect automatically the onsets of greenup (greenness starts to increase), maturity (greenness approaches maximum), senescence (greenness begins to decrease), and dormancy (greenness reaches a minimum) (Zhang *et al* 2003). Finally, the growing season amplitude in NDVI ($NDVI_{AMP}$) is calculated from the difference between the NDVI value at the onset of greenup and the onset of maturity. The growing season aggregated NDVI ($NDVI_{AGG}$) is computed by summing the fitted daily NDVI values throughout the period between the greenup onset and the dormancy onset. These two greenness parameters ($NDVI_{AMP}$ and $NDVI_{AGG}$) minimize the impact of systematic uncertainty in the long time series of NDVI data and remove the influence of seasonal shifts in vegetation growth. Note that vegetation greenness in 1994 is not calculated because there are no AVHRR observations from August to December.

2.2. Precipitation data and dry season length

Precipitation data were used to investigate the responses of vegetation greenness to rainfall variations. Three-hourly precipitation data were obtained at a spatial resolution of 32 km (approximately 0.25°) between 1981 and 2007 from the NOAA

NCEP (National Centers for Environmental Prediction) North America Regional Reanalysis (NARR) (Mesinger *et al* 2006) and are aggregated to daily values. This dataset provides the most accurate and consistent long time series of precipitation that covers North America (Mesinger *et al* 2006). Evaluation of this dataset indicates that the NARR precipitation provides a good representation of the spatial distribution, diurnal cycle, and annual cycle of precipitation and is superior to the other reanalyses over the contiguous United States (Bukovsky and Karoly 2007). It also captures extreme events well, even over western topography. Some uncertainties are caused by model ingestion of precipitation observations, and data outside of the contiguous United States may be less accurate (Bukovsky and Karoly 2007).

This precipitation dataset is applied to calculate annual precipitation and maximum dry season length, where annual precipitation is a simple summation of daily data. To determine maximum dry season length, a dry episode is defined as the number of consecutive days during which the cumulative daily precipitation is less than 10% of the mean annual rainfall in an individual pixel. Thus, a set of dry episodes within a year are generated by moving a one-day step along the time series of daily rainfall data in the given year, including an extension of the preceding half years. In this way, we also capture dry episodes that cover parts of two calendar years. By comparing the extracted dry episodes, the maximum consecutive dry duration within a year before the end of the vegetation growing season is calculated to represent the dry season length.

2.3. Interannual trend detections in both vegetation greenness and precipitation

Trends in the vegetation greenness and precipitation time series are quantified using linear regression trends and are calculated for individual pixels and ecosystems, respectively, during different time periods. The ecosystems we focused on here are dryland ecosystems that include IGBP (International Geosphere–Biosphere Programme) land cover type open shrublands, close shrublands, barren-sparsely-vegetated lands, and grasslands (figure 1). Croplands, savannas, and forests are excluded from the analyses. At the ecosystem level, time series of vegetation greenness and precipitation data are spatially averaged. Before trend analysis, the interannual time series at both the pixel and ecosystem levels are smoothed using a three-step moving window average to reduce statistical uncertainties caused by the first and last values and individual outliers in the temporal pattern. The significance of temporal trends was tested using a one tailed test.

Further, the percentage of greenness change in a given period is determined by comparing the calculated difference from the regression trend with the long-term mean. Moreover, after calculating the trend for each pixel, the regions with severe drought stress, which were defined based on the smallest $NDVI_{AGG}$ and annual precipitation in the long-term time series, are extracted by comparing differences in the trends in each state over the western United States (US) and Mexico.

Controls of precipitation on vegetation growth are investigated by analyzing statistical correlations between

Table 1. Relative changes in vegetation greenness in various periods (negative values denote decreasing trend and N/A represents no significant trend).

|	1982–1993		1993–2007		1993–2002		1982–2007	
	$\mathrm{NDVI_{AGG}}$ (%)	$\mathrm{NDVI_{AMP}}$ (%)	$\mathrm{NDVI_{AGG}}$ (%)	$\mathrm{NDVI_{AMP}}$ (%)	$\mathrm{NDVI_{AGG}}$ (%)	$\mathrm{NDVI_{AMP}}$ (%)	$\mathrm{NDVI_{AGG}}$ (%)	$\mathrm{NDVI_{AMP}}$ (%)
Shrublands	21.0	8.9	−6.1	−10.8	−15.8	−16.9	N/A	−7.1
Grasslands	26.3	11.5	−13.5	−24.7	−20.9	−24.0	8.1	N/A

vegetation greenness and precipitation time series. To examine interannual variation, greenness in growing season is correlated to both annual precipitation and dry season length using multiple (stepwise) linear regression after the data were re-projected and aggregated to a spatial resolution of 0.25° (equivalent to the resolution of NARR data). Further, seasonal responses of greenness to precipitation are investigated using four-week data (i.e. roughly to monthly data) from 1982 to 2007. The time series used for seasonal analysis consists of 338 pairs of samples in each 0.25° grid. Because of the time lag between vegetation greenness and precipitation (e.g., Nicholson and Farrar 1994, Potter and Brooks 1998, Schultz and Halpert 1993, Wang *et al* 2003), four-week NDVI greenness is compared with four-week precipitation at thirteen different time lags (0–12 biweekly periods). This allows us to assess the timescale of precipitation that most strongly influences vegetation greenness.

3. Results

### 3.1. Regional and ecosystem trends in vegetation greenness

Vegetation greenness shows complex temporal trends in both grasslands and shrublands over last 26 years. The standard deviation in the area-averaged greenness was relatively stable each year. The standard deviation of $\mathrm{NDVI_{AMP}}$ ranges varies from 0.066 to 0.080 and from 0.071 to 0.084 in grasslands and shrublands, respectively. The $\mathrm{NDVI_{AGG}}$ standard deviation varies from 0.26 to 0.29 and from 0.19 to 0.26 in grasslands and shrublands, respectively. Although the standard deviation suggests that the spatial variation is substantial, the average greenness reveals general trends related to interannual vegetation changes. The overall trend shows that $\mathrm{NDVI_{AGG}}$ in shrublands (mainly distributed west of the Rocky Mountains) presents no statistically significant change, while $\mathrm{NDVI_{AMP}}$ significantly decreased by 7.1% ($p <$ 0.01) (figure 3(a)). In contrast, $\mathrm{NDVI_{AGG}}$ increased by 8.1% ($p < 0.05$) in grasslands (mainly distributed between the central US and the Rocky Mountains), while $\mathrm{NDVI_{AMP}}$ shows insignificant changes. This suggests that overall greenness shows a positive trend in grasslands but a negative trend in shrublands. Note that $\mathrm{NDVI_{AGG}}$ represents vegetation growth integrated over growing season while $\mathrm{NDVI_{AMP}}$ reflects the maximum greenness. Thus, these two parameters are both necessary to summarize patterns in vegetation dynamics.

A close examination of the time series of greenness reveals that vegetation greenness shows evidence of longer term cycles. Generally, vegetation growth (as represented by $\mathrm{NDVI_{AGG}}$) increased from 1982 to 1993 then transitioned
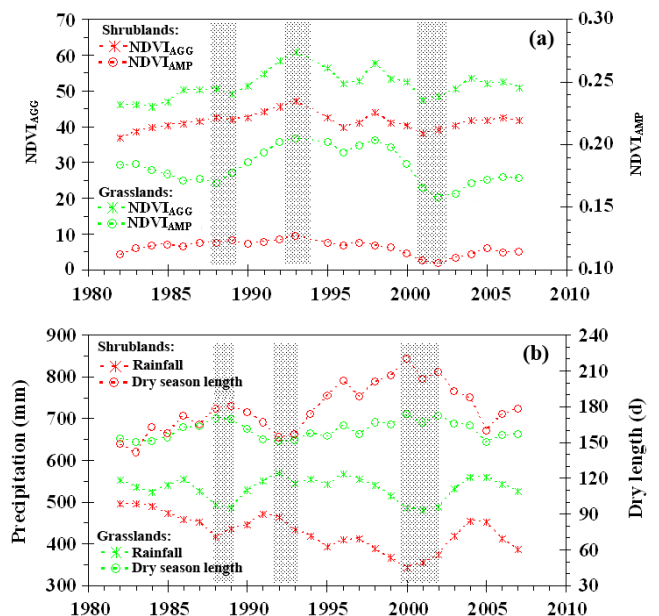

Figure 3. Time series of spatially averaged vegetation greenness and precipitation characteristics from 1982 to 2007. (a) $\mathrm{NDVI_{AMP}}$ and $\mathrm{NDVI_{AGG}}$; (b) annual precipitation and dry season length. The vertical bands highlight the local peaks and valleys in the time series.

to a decreasing trend from 1993 to 2007 (figure 3(a)). A greenness peak appears around 1993, while local minima occur in 1988/1989 and 2000/2001. Other weak cycles also exist within short time periods.

The cycle is much stronger in grasslands than in shrublands (figure 3(a) and table 1). From 1982 to 1993, $\mathrm{NDVI_{AGG}}$ increased by 26.3% of the 26 year average in grasslands and 21.0% in shrublands. From 1993 to 2007, however, $\mathrm{NDVI_{AGG}}$ decreased by 13.5% in grasslands and by 6.1% in shrublands. The strongest linear trend occurred in 1993–2001/2002, when $\mathrm{NDVI_{AGG}}$ decreased by 20.9% in grasslands and 15.8% in shrublands. Similar trends appear in $\mathrm{NDVI_{AMP}}$ during these periods (figure 3(a) and table 1). The spatial pattern of $\mathrm{NDVI_{AMP}}$ in two extreme years highlights the regions with the most severe drought impacts (figures 4(a)–(c)). The $\mathrm{NDVI_{AMP}}$ is distinctly larger in 1993 than that in 2001 across the region, particularly in grasslands in the eastern region. Note that the strong reduction of greenness in shrublands may reflect accumulated drought impacts over several years because of interannual memory effects (Richard *et al* 2008). This pattern presents the range of vegetation greenness varying between optimal and severe dry years. In other words, the range provides the magnitude of vegetation reduction caused by severe drought stress.
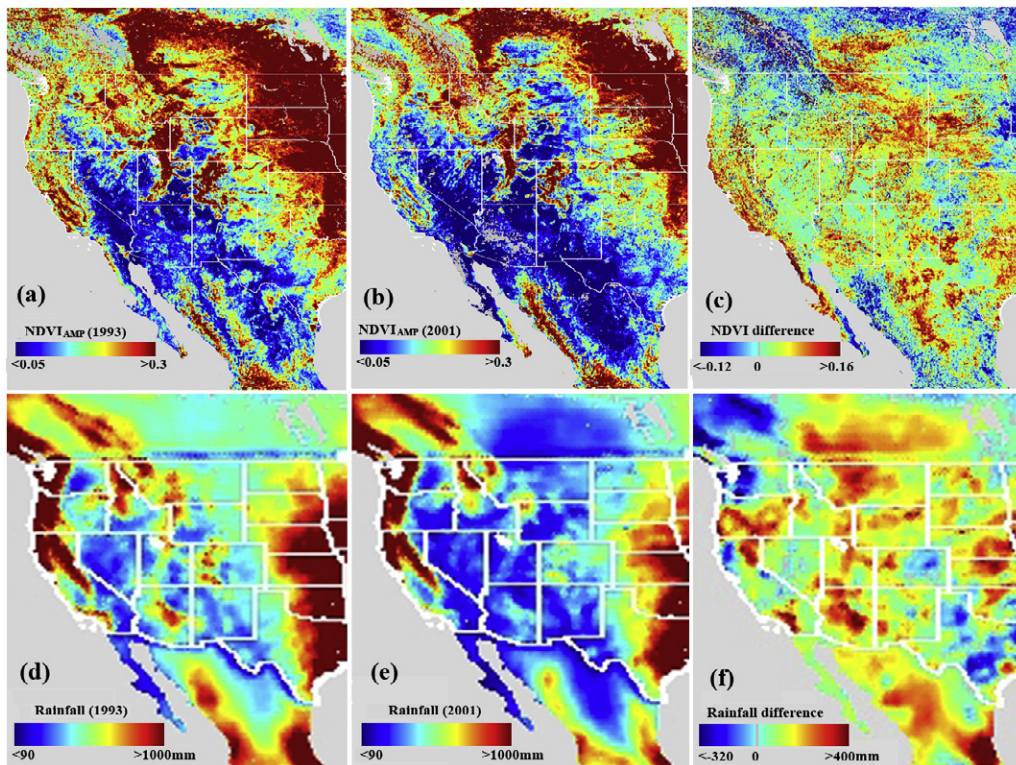
Figure 4. Comparison of spatial patterns in NDVI$_{AMP}$ and annual rainfall in the wet year (1993) and the dry year (2001). (a) NDVI$_{AMP}$ in 1993; (b) NDVI$_{AMP}$ in 2001; (c) NDVI$_{AMP}$ difference between 1993 and 2001; (d) annual rainfall in 1993; (e) annual rainfall in 2001; and (f) the difference in annual rainfall between 1993 and 2001.
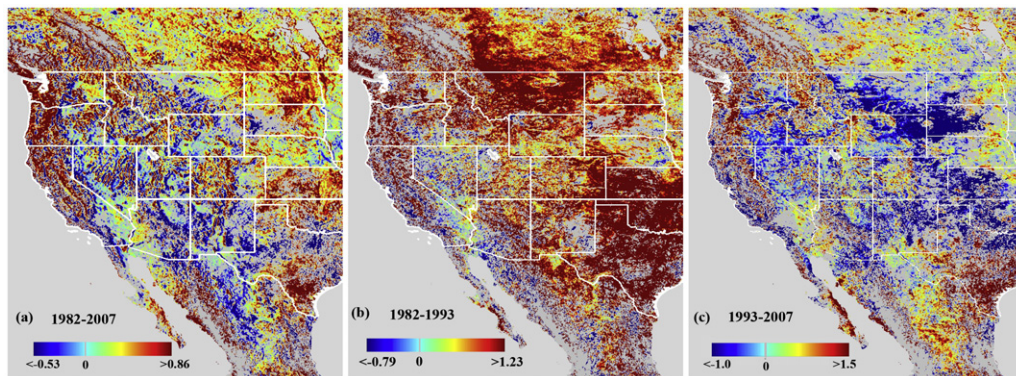

Figure 5. Spatial pattern in NDVI$_{AGG}$ trend (NDVI/year) across southwestern NA in different time periods ($p < 0.1$).

3.2. Spatiotemporal complexity in vegetation greenness trends

Trends in local vegetation greenness vary substantially across southwestern North America (figure 5). From 1982 to 2007, NDVI$_{AGG}$ in the majority of areas in the study region exhibited significant increases or non-significant changes; however, reduction in NDVI$_{AGG}$ occurs in more than one third of the area of Arizona, Nevada, New Mexico, and Utah (figures 5(a) and 6(a)). Similarly, NDVI$_{AGG}$ is lower in about 20% of California, Idaho, and Wyoming. Trends towards lower values are much stronger in NDVI$_{AMP}$, and account for 40–60% of the areas in each state, except for the eastern part of the study region, such as South Dakota, North Dakota, and Montana (figure 6(b)).

The multi-year cycles in vegetation trends vary considerably across the study region. From 1982 to 1993, NDVI$_{AGG}$ increased significantly in more than 60% of the eastern part of the study region (Kansas, Montana, and the Dakotas) (figures 5(b), 6(c) and (d)), but increased in less than 45% of area in the western region, particularly in Arizona, California, and Nevada. NDVI$_{AMP}$ changed significantly in about 50% of the study area, with 34% of the area showing significant increasing trends, and 15% exhibiting decreasing trends. Lower NDVI$_{AMP}$ occurs in about 24.5% of the western region.

Vegetation generally exhibits patterns of increasing and decreasing greenness that are less geographically extensive
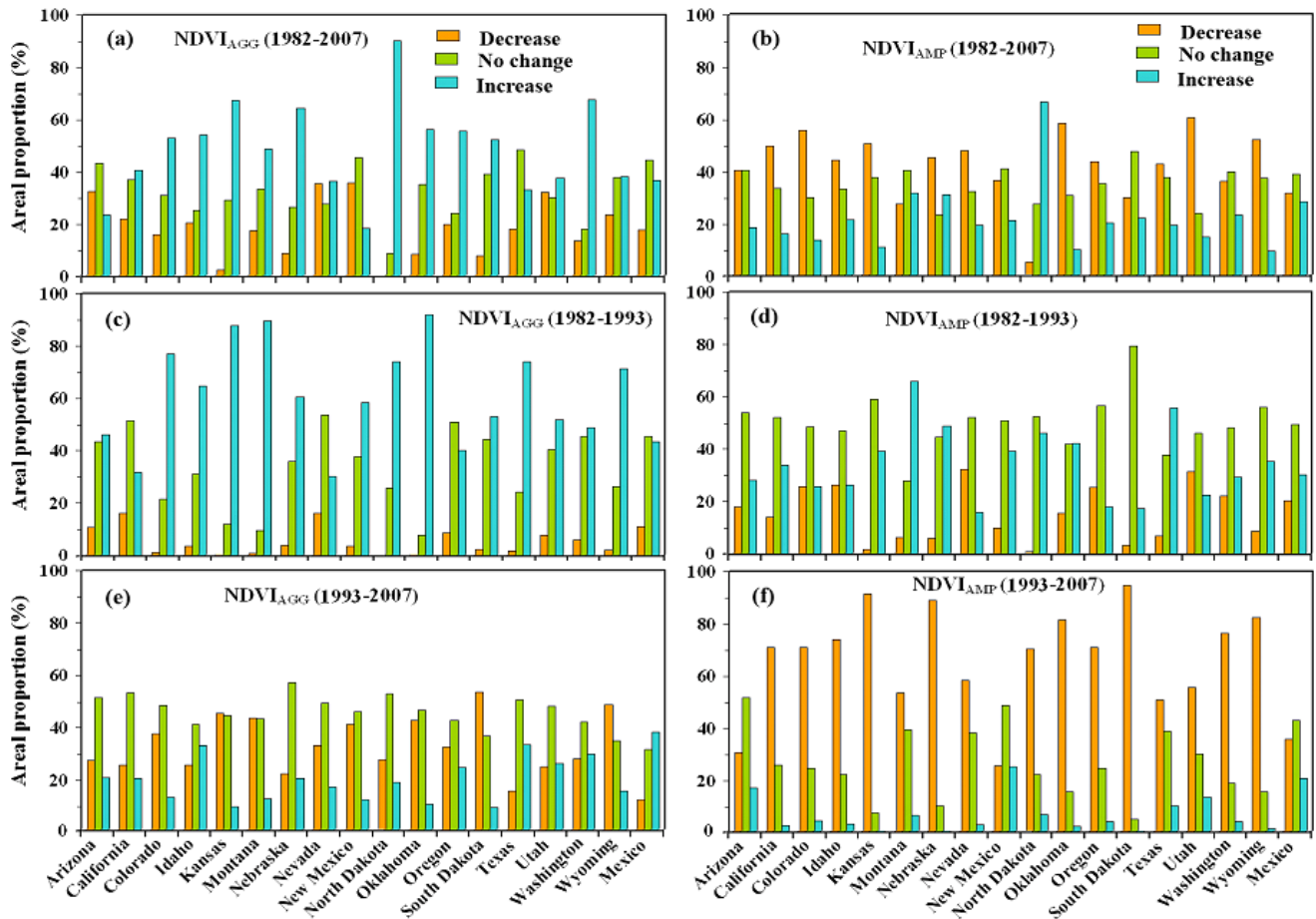
Figure 6. Proportion of area with different greenness trends (significance level *p* < 0.1) in various US states and Mexico from 1982 to 2007, and from 1982 to 1993, 1993 to 2007, separately.

(*p* < 0.1) during the subsequent period from 1993 to 2007 (figures 5(c), 6(e) and (f)). The overall areal proportion for changes in NDVI$_{AGG}$ are: 21% increasing, 33% decreasing, and 46% experiencing no significant change (figures 5(c) and 6(e)). Areas with decreasing values are concentrated (>40% of areas) in Kansas, Montana, New Mexico, Oklahoma, South Dakota, and Wyoming; mainly east of the Rockies. A similar spatial pattern is revealed in NDVI$_{AMP}$, but the decrease is even more pronounced. Specifically, NDVI$_{AMP}$ showed 7%—increase, 66%—decrease, and 27%—no-change.

The above patterns in greenness in each state are associated with the specific ecosystems. Grasslands or shrublands tend to be dominant in any given state (figures 1 and 7). For example, shrublands cover 83%, 75%, and 63% of the lands in Arizona, Nevada, and New Mexico, respectively. In contrast, grasslands account for 79%, 66%, and 62% in Wyoming, Oklahoma, and Montana, respectively.

3.3. Dependence of greenness on precipitation and dry season length

Vegetation greenness in the study region strongly depends upon the annual cycle of rainfall. The dry season length from 1982 to 2007, on average, increased by 1.6 days year^{-1} (*p* < 0.001) in shrublands (western region), but exhibits a
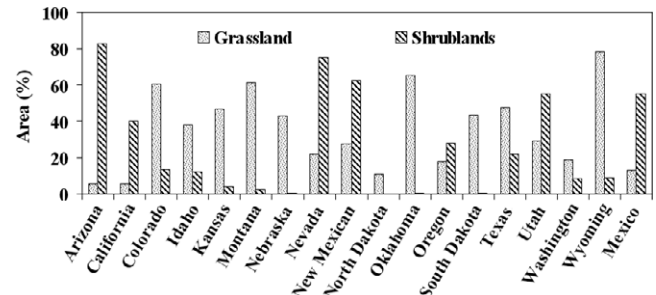

Figure 7. Proportion of grasslands and shrublands in each state.

much weaker overall trend (0.3 days year^{-1}, *p* < 0.10) in grasslands (eastern region) (figures 3(b) and 8(b), table 2). However, inspection of time series presents two apparent cycles in growing season length. The first cycle occurs from 1982 to 1992/1993 with a peak occurring around 1988/1989. The second cycle is from 1993 to 2005 with a peak at 2000–2002 (figure 3(b)). The range of variation in dry season length within each of these cycles is about 20 days in grasslands. In contrast, the range in shrublands is about 40 days in the first cycle and 60 days in the second cycle. This suggests that the period of vegetation drought stress increased in shrublands

Table 2. Interannual variation in annual rainfall (mm year^{-1}) and dry seasonal length (day year^{-1}) in various periods (negative value denotes decreasing trend and N/A represents no significant trend).

	1982–1993		1993–2007		1993–2002		1982–2007	
	Rainfall	Dry length	Rainfall	Dry length	Rainfall	Dry length	Rainfall	Dry length
Shrublands	−4.61	1.22	N/A	N/A	−8.47	5.02	−3.82	1.56
Grasslands	N/A	N/A	−1.31	N/A	−9.31	2.24	N/A	0.27
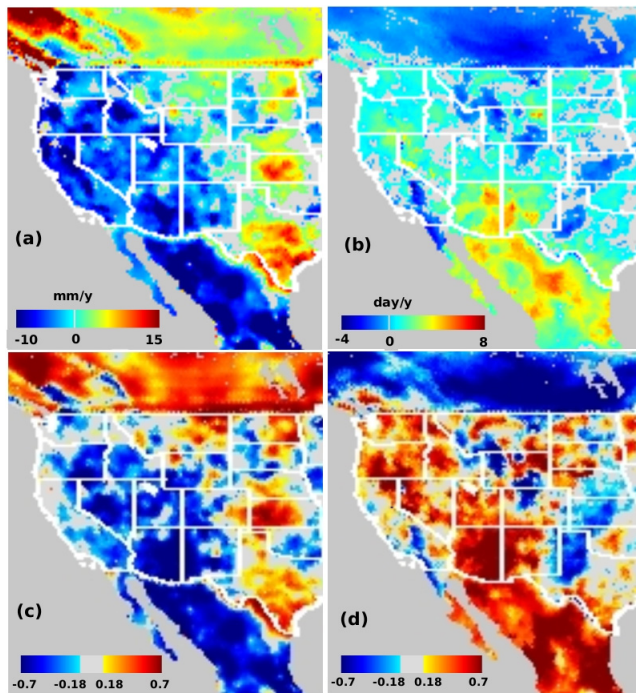
Figure 8. Spatial pattern of interannual trends in rainfall characteristics from 1981 to 2007. (a) Change rate of annual rainfall (mm year^{-1}), (b) change rate of dry season length (days year^{-1}), (c) correlation coefficient of rainfall against time, and (d) correlation coefficient of dry season length against time. Note that there are artifacts in the rainfall data around the boundary of different countries.

and that the drought was spread over several years with shrubs decreasing in density.

Multi-year cycles in rainfall patterns are also evident, although the timing of rainfall maxima and minima are opposite to those of dry season length. Annual rainfall in shrublands decreased significantly at a rate of 4 mm year^{-1} ($p < 0.0005$) from 1982 to 2007 and with no significant overall change from 1993 to 2007 (table 2). Within this 26 year period, annual rainfall in shrublands oscillated between peaks around 1992/1993 and 2005, and minima around 1988 and 2000/2001 (figure 3(b)). Similar patterns are observed in grasslands (table 2 and figure 3(b)), where rainfall decreased 1.3 mm year^{-1} ($p < 0.15$) from 1993 to 2007.

The spatio-temporal patterns in rainfall and dry season length show great geographical variability from 1981 to 2007 (figure 8). In the western region (shrublands), rainfall decreased significantly ($p < 0.2$) at a rate of 1–10 mm year^{-1}. Correspondingly, dry season length increased at a rate as large as 8 days year^{-1}. In contrast, trends in both rainfall and dry
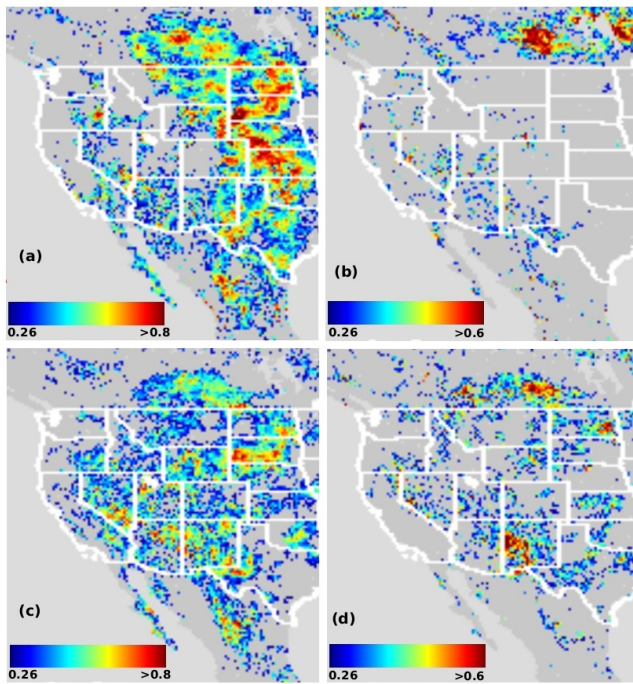
season length vary with local conditions in the eastern region (grasslands), which could be increased, decreased, or have no significant changes. Indeed, drought conditions have been much more severe in the western region than in the eastern region during the last 26 years. This suggests progressive aridification, particularly over the western region, although the drought intensity exhibits episodic behavior.

These interannual variations in rainfall and dry season length correlate to patterns in vegetation greenness at multiple time scales. Specifically, the observed cycles in rainfall covary with those of greenness (figure 3). Although the trends in rainfall and dry season length over some short periods are not significant, they are similar to the observed greenness trends. However, the rainfall and greenness from 1982 to 1993 in shrublands do not match well. This is likely associated with the complex response of shrubs to rainfall, including memory effects (Pavón and Briones 2001, Richard *et al* 2008). Moreover, the spatial pattern in vegetation greenness in both the wettest and driest years (figures 4(a)–(c)) match well with the corresponding pattern in precipitation (figures 4(d) and (e)).

3.4. Correlation between vegetation greenness and rainfall

Correlation between annual vegetation growth and rainfall quantitatively indicates the vegetation response to climate changes. Spatial averages indicate that NDVI$_{AGG}$ and NDVI$_{AMP}$ are significantly and positively correlated with annual precipitation ($p < 0.01$ in grasslands and $p < 0.05$ in shrublands) and are negatively correlated with dry season length ($p < 0.05$) in both grasslands and shrublands. At the grid (0.25°) level, NDVI$_{AGG}$ shows strongly significant correlation with annual rainfall and less significant correlation with dry season length in grasslands (figures 9(a) and (b)). In contrast, NDVI$_{AMP}$ correlates positively to precipitation and negatively to dry season length in both grasslands and shrublands (figures 9(c) and (d)).

Vegetation growth appears to be a function of both rainfall amount and dry season length. The relationship (stepwise regression) between vegetation growth and the linear combination of annual precipitation and dry season length is significant over much of the region (figure 10). Evidently, the linear combination of rainfall and dry season duration explains interannual variation in NDVI$_{AGG}$ and NDVI$_{AMP}$ better than either individual rainfall parameter. Across the region, NDVI$_{AGG}$ responds to precipitation and dry season length more significantly in grasslands ($r > 0.5$) than in shrublands ($r < 0.5$) while NDVI$_{AMP}$ responds similarly in both ecosystems (figure 10). The NDVI$_{AGG}$ response is likely associated with the fact that grasses are more sensitive to rainfall conditions while shrubs are relatively drought resistant

Figure 9. Correlation coefficient ($p < 0.2$) for NDVI$_{AGG}$ and rainfall (a), NDVI$_{AGG}$ and dry season length (negative correlation) (b); NDVI$_{AMP}$ and rainfall (c); NDVI$_{AMP}$ and dry season length (negative correlation) (d).

parts of Mexico. The high correlation suggests that seasonal cycles in precipitation and greenness are comparable and the short lag indicates that rainfall rapidly triggers the emergence of grasses and strongly controls grass growth in these areas. In contrast, the correlation between four-week greenness and precipitation in shrublands of western North America are relatively weak (maximum $r < 0.4$, $p < 0.05$). The maximum correlation coefficient occurs when greenness is compared with precipitation in the preceding one or two months. The large lag indicates vegetation greenness in shrubs responds slowly to precipitation and large greenness does not necessary correspond to large amounts of precipitation in a four-week period. This suggests that the relationship between seasonal greenness and precipitation in shrublands is complex (Pavón and Briones 2001) and may reflect the effects of memory in shrubs to preceding rainfall (Richard *et al* 2008).

4. Discussion

Spatio-temporal patterns in vegetation greenness present a very complex pattern in response to periodic drought and rainfall conditions. Across southwestern North America, vegetation growth is primarily dependent upon winter precipitation in the western region, while in the southern and eastern regions, it depends on precipitation received during the summer season (Arizona 'Monsoon') (Hanson and Weltzin 2000). Different climate regimes produce spatial variations in vegetation growth. The significant decrease in greenness from 1982 to 2007 mainly appears in the western regions. In contrast, the decreasing NDVI$_{AGG}$ from 1993 to 2007 is dominant in the eastern part of the study region. Understanding these local impacts caused by moisture stress on vegetation growth is critical for mitigating and adapting to the threat of climate changes (Giorgi *et al* 2008).

Vegetation greenness trends in most parts of southwestern North America are generally episodic rather than persistant in response to climate changes. Monotonically increasing NDVI$_{AGG}$ have been widely reported in northern mid-high latitudes because of warming temperatures (Myneni *et al* 1997, Zhou *et al* 2001, Zhang *et al* 2007) and in arid-semiarid

and tolerant to modest variability in precipitation regimes. The NDVI$_{AMP}$ values are likely to be influenced by single rainfall events. Figure 10 also illustrates the diverse geographic responses to variation in the precipitation amount and drought stress.
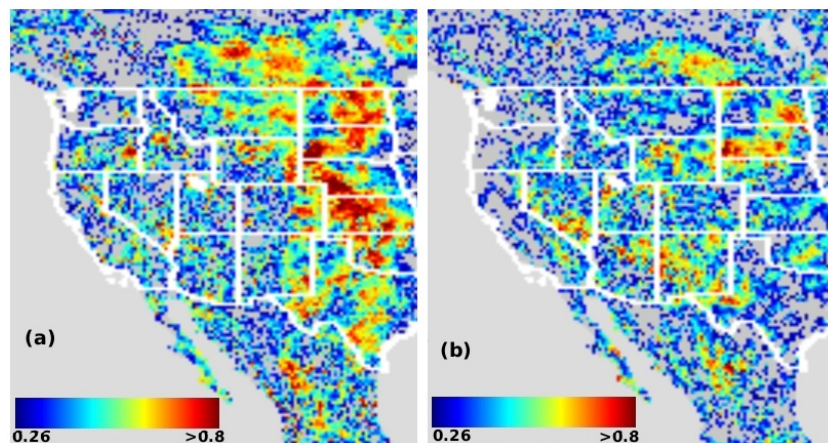
Seasonal vegetation growth is also significantly controlled by seasonal-scale precipitation regimes (figure 11). Specifically, timing in seasonal greenness shows substantial lag in its response to precipitation across the region. Four-week NDVI greenness is significantly correlated with precipitation ($r > 0.7$, $p < 0.01$) in most grasslands, with a lag less than two weeks. A similar relationship is found for shrublands in

Figure 10. Correlation coefficient obtained from stepwise regression. NDVI$_{AGG}$ (a) and NDVI$_{AMP}$ (b) correlated with both annual rainfall and dry season length.
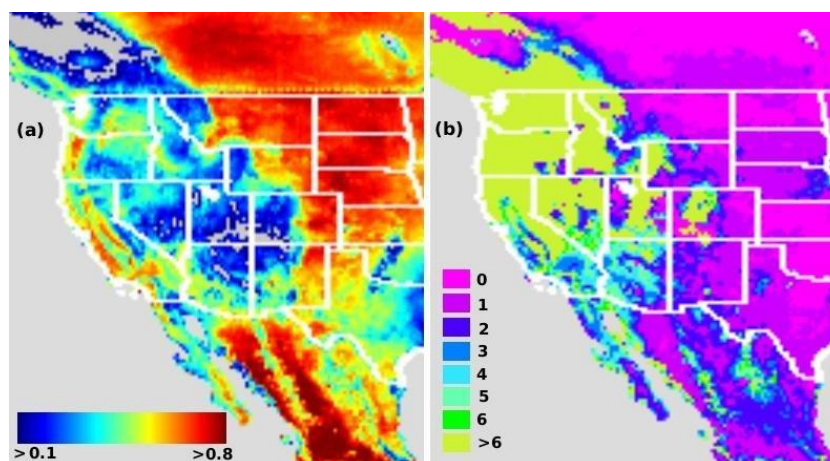
Figure 11. Correlations between four-weekly NDVI and precipitation from 1982 to 2007. (a) The maximum correlation coefficient ($p < 0.05$) occurs at the time lag (b), and (b) the value indicates the number of two weeks.

environments because of more frequent precipitation, such as in the Sahel (Olsson *et al* 2005), over Western China (Piao *et al* 2006), Asia (Lee *et al* 2008), and monsoonal northern Australia (Bowman *et al* 2008). However, because southwestern North America is characterized by periodic drought (Hanson and Weltzin 2000, Groisman and Knight 2008), vegetation greenness is more likely to exhibit complex cycles. Our results demonstrate that rainfall in the study region was characterized by a long term cycle that peaked around 1993 and with severe droughts in 1988/1989 and 2000–2002 (figure 3). In response, vegetation greenness consistently followed the above temporal cycle and was significantly correlated to rainfall and dry season length, respectively. Most importantly, vegetation greenness is dependent upon the combination of both precipitation and dry season length. This result arises from the fact that extreme rainfall events, which have been increasing over the last half century (Peterson *et al* 2008), increase the amount of annual precipitation and runoff (Maraun *et al* 2008), but have limited benefit to vegetation growth (Schultz and Halpert 1993, Nicholson and Farrar 1994). In these cases, dry season length plays a more significant role in limiting vegetation growth.

Vegetation greenness has decreased substantially in recent decades across southwestern North America and over the last 26 years in the westernmost parts of the study region. This trend is likely to continue because of the influence of prolonged drought. The percentage of dry day episodes has increased by 3.1%–4.3% during the past 40 years (Groisman and Knight 2008) and seasonal precipitation shows slightly negative trends in the southwestern US (Livezey *et al* 2007), although heavy precipitation and daily precipitation on average across North America has been increasing over the last half century (Peterson *et al* 2008). Furthermore, the IPCC (2007) reports that the intensity and frequency of droughts are expected to increase in this region, and a recent analysis of 19 models concludes that the southwestern US has transitioned to a more arid climate and that this trend will continue in the 21st century (Seager *et al* 2007). Consequently, aridification will likely continue to cause reduction of vegetation greenness and could lead to changes in ecological communities, including

the spread of alien species (Walther *et al* 2002). Based on the results presented in this study, any longer term trends in vegetation are likely to follow multi-year oscillations instead of a consistent linear trend.

Reduction in vegetation greenness has led to decreases in carbon uptake across southwestern North America since 1993, and some western regions since 1982. Because $NDVI_{AGG}$ provides a strong proxy of ecosystem primary productivity and changes in CO_2 flux (e.g., Posse and Cingolani 2004, Tucker *et al* 1986, Goetz *et al* 2005, Myneni and Williams 1994, Goetz and Prince 1999, La Puma *et al* 2007), trends in $NDVI_{AGG}$ should capture the relative variation in CO_2 uptake by photosynthesis. Thus, we can expect that overall, CO_2 uptake has decreased slightly in shrublands while it has increased in grasslands during the last 26 years. Drought stress during 1993–2007 has likely resulted in reduced CO_2 uptake in grasslands and shrublands. As indicated in the $NDVI_{AGG}$ trend from 1993 to 2002, severe drought could strongly reduce CO_2 uptake in both grasslands and shrublands (figure 4). This reduced uptake implies that this drought stress could be resulting in a significant source of atmospheric CO_2.

5. Conclusions

Long-term AVHRR data and daily rainfall data provide a means to investigate vegetation responses to climate changes in drylands across southwestern North America. Seasonal response of vegetation growth to climate change is revealed by four-week NDVI and precipitation data. Seasonal greenness in grasslands is strongly dependent on seasonal precipitation, with a time lag less than two weeks. In contrast, seasonal greenness in some shrublands responds to seasonal precipitation slowly and less strongly, with a lag of about one to two months. The growing season amplitude and summation of NDVI, which are derived from the vegetation phenological trajectory, are robust parameters that provide useful information related to interannual variation in vegetation growth. Greenness data from 1982 to 2007 reveal that vegetation in southwestern North America exhibited multiple

growth cycles during this period. Overall, the NDVI$_{AGG}$ increased by more than 20% and NDVI$_{AMP}$ increased by about 10% from 1982 to 1993 across the region. In contrast, both NDVI$_{AGG}$ and NDVI$_{AMP}$ decreased from 1993 to 2007. This decreasing trend was much stronger in grasslands than in shrublands. Because of covariance between greenness and precipitation, drought stress is likely the main factor reducing vegetation growth across the region. The maximum amplitude in the interannual greenness cycle indicates that severe drought stress reduced NDVI$_{AGG}$ by 16% in shrublands and 21% in grasslands and reduced NDVI$_{AMP}$ by 17% and 24% in these two ecosystems, respectively.

Spatial patterns in greenness dynamics highlight the local patterns in vegetation changes. From 1982 to 2007, reduction in NDVI$_{AGG}$ occurs in more than one third of Arizona, Nevada, New Mexico, and Utah, and in about 20% of California, Idaho, and Wyoming. From 1993 to 2007, strong decreasing trends appear in more than 40% of the area in Kansas, Montana, New Mexico, Oklahoma, South Dakota, and Wyoming. The area with lower NDVI$_{AMP}$ is much larger in several states. Local patterns in greenness reduction may indicate the effects of decreased rainfall in specific regions, which could help policy makers to manage the ecological status and natural resources of these lands.

Dynamics in vegetation greenness in southwestern North America are strongly dependent on rainfall and dry season length. Multi-year cycles in vegetation greenness coincide well with cycles in annual rainfall and dry duration, separately. However, stepwise regression in each grid cell ($0.25°$) indicates that vegetation greenness is a function of both annual rainfall and dry season duration. This suggests that the complex spatiotemporal responses of vegetation greenness to changes in annual rainfall and dry duration are likely to result in changes to vegetation community structure, ecosystem functioning, fire regime, and species composition. The results also highlight that the combination of rainfall and dry season length plays a significant role with far-reaching consequences for ecosystem and biosphere functioning and structure. Because the trend toward more frequent and intense droughts in this region is likely to continue, it will increase the severity of ecosystem degradation and further reduce vegetation greenness and carbon uptake.

The detection of vegetation phenology and greenness in arid and semiarid environments is much more complex than in other ecosystems. Thus, the results presented in this letter represent general spatial patterns and trends in vegetation greenness in response to climate changes. Further research is needed to investigate the accuracy of NDVI$_{AGG}$ and NDVI$_{AMP}$ for individual pixels.

Acknowledgments

References

Bowman D M J S, Riley J E, Boggs G S, Lehmann C E R and Prior L D 2008 Do feral buffalo (*Bubalus bubalis*) explain the increase of woody cover in savannas of Kakadu National Park, Australia? *J. Biogeogr.* **35** 1976–88

Bukovsky M S and Karoly D J 2007 A brief evaluation of precipitation from the North American regional reanalysis *J. Hydrometeorol.* **8** 837–46

Cook C D and Heerdegen R G 2001 Spatial variation in the duration of the rainy season in monsoonal Australia *Int. J. Climatol.* **21** 1723–32

Donahue D R, Sapper J, Heidinger A, Jelenak A and Kapoor V 2005 CLAVR-x initial operational capability at NESDIS *21st Int. Conf. on Interactive Information and Processing Systems (IIPS) for Meteorology, Oceanography, and Hydrology (San Diego, CA, Jan. 2005)* (Boston, MA: American Meteorological Society) paper 10.2

Fauchereau N, Trzaska S, Rouanlt M and Richard Y 2003 Rainfall variability and changes in southern Africa during the 20th century in the global warming context *Nat. Hazards* **29** 139–54

Fuller D O and Prince S D 1996 Rainfall and foliar dynamics in tropical southern Africa: potential impacts of global climatic change on savanna vegetation *Clim. Change* **33** 69–96

Giorgi F *et al* 2008 The regional climate change hyper-matrix framework *EOS Trans. Am. Geophys. Union* **89** 445–6

Goetz S J, Bunn A G, Fiske G and Houghton R A 2005 Satellite observed photosynthetic trends across boreal North America associated with climate and fire disturbance *Proc. Natl Acad. Sci.* **102** 13521–5

Goetz S J and Prince S D 1999 Modeling terrestrial carbon exchange and storage: the evidence for and implications of functional convergence in light use efficiency *Adv. Ecol. Res.* **28** 57–92

Goward S N, Tucker C J and Dye D G 1985 North American vegetation patterns observed with the NOAA-7 advanced very high resolution radiometer *Plant Ecol.* **6** 3–14

Groisman P Y A and Knight R W 2008 Prolonged dry episodes over the conterminous United States: new tendencies emerging during the last 40 years *J. Clim.* **21** 1850–62

Gutman G, Tarpley D, Ignatov A and Olson S 1995 The enhanced NOAA global land datasets from the advanced very high resolution radiometer *Bull. Am. Meteorol. Soc.* **76** 1141–56

Hansen J M, Sato R, Ruedy K, Lo D, Lea W and Medina-Elizade M 2006 Global temperature change *Proc. Natl Acad. Sci.* **103** 14288–93

Hanson P J and Weltzin J F 2000 Drought disturbance from climate change: response of United States forests *Sci. Total Environ.* **262** 205–20

IPCC 2007 *Climate Change 2007: Impacts, Adaptation, and Vulnerability* Contribution of Working Group II to the Fourth Assessment Report of the Intergovernment Panel on Climate Change, ed M L Parry, O F Canziani, J P Palutikof, P J van der Linden and C E Hanson (Cambridge: Cambridge University Press) 976pp

Justiniano M J and Fredericksen T S 2000 Phenology of tree species in Bolivian dry forests *Biotropica* **32** 276–81

Kogan F, Gitelson A, Zakarin E, Spivak L and Lebed L 2003 AVHRR-based spectral vegetation index for quantitative assessment of vegetation state and productivity: calibration and validation *Photogramm. Eng. Remote Sens.* **69** 899–906

Kramer K, Leinonen I and Loustau D 2000 The importance of phenology for the evaluation of impact of climate change on growth of boreal, temperate and Mediterranean forests ecosystems: an overview *Int. J. Biometeorol.* **44** 67–75

La Puma I P, Philippi T E and Oberbauer S F 2007 Relating NDVI to ecosystem CO$_2$ exchange patterns in response to season length and soil warming manipulation in arctic Alaska *Remote Sens. Environ.* **109** 225–36

Lee E, Chase T N and Rajagopalan B 2008 Highly improved predictive skill in the forecasting of the East Asian summer monsoon *Water Resources Res.* **14** W10422

Livezey R E, Vinnikov K Y, Timofeyeva M M, Tinker R and van den Dool H M 2007 Estimation and extrapolation of climate normals and climatic trends *J. Appl. Meteor. Climatol.* **46** 1759–76

Lotsch A, Friedl M A, Anderson B T and Tucker C J 2003 Coupled vegetation-precipitation variability observed from satellite and climate records *Geophys. Res. Lett.* **30** 1774

Lotsch A, Friedl M A, Anderson B T and Tucker C J 2005 Response of terrestrial ecosystems to recent Northern Hemispheric drought *Geophys. Res. Lett.* **32** L06705

Maraun D, Osborn T J and Gillett N P 2008 United Kingdom daily precipitation intensity: improved early data, error estimates and an update from 2000 to 2006 *Int. J. Climatol.* **28** 833–42

Martiny N, Richard Y and Camberlin P 2005 Interannual persistence effects in vegetation dynamics of semi-arid Africa *Geophys. Res. Lett.* **32** L24403

MEA (Millennium Ecosystem Assessment) 2005 *Ecosystems and Human Well-Being: Desertification Synthesis* (Washington, DC: World Resources Institute) p 26

Mesinger F *et al* 2006 North American regional reanalysis *Bull. Am. Meteorol. Soc.* **87** 343–60

Myneni R B and Williams D L 1994 On the relation between FAPAR and NDVI *Remote Sens. Environ.* **49** 200–11

Myneni R B *et al* 1997 Increased plant growth in the northern high latitudes from 1981–1991 *Nature* **386** 698–702

Nemani R R, Keeling C D, Hashimoto H, Jolly W M, Piper S C, Tucker C J, Myneni R B and Running S W 2003 Climate-driven increases in global terrestrial net primary production from 1982 to 1999 *Science* **300** 1560–3

Nicholson S E and Farrar T J 1994 The influence of soil type on the relationships between NDVI, rainfall, and soil moisture in semiarid Botswana. I. NDVI response to rainfall *Remote Sens. Environ.* **50** 107–20

Olsson L, Eklundh L and Ardö J 2005 Greening of the Sahel—trends, patterns and hypotheses *J. Arid Environ.* **63** 556–66

Pavón N P and Briones O 2001 Phenological patterns of nine perennial plants in an intertropical semi-arid Mexican scrub *J. Arid Environ.* **49** 265–77

Peñuelas J, Filella I, Zhang X Y, Llorens L, Ogaya R, Lloret F, Comas P, Estiarte M and Terradas J 2004 Complex spatiotemporal phenological shifts as a response to rainfall changes *New Phytol.* **161** 837–46

Peterson T C, Zhang X, Brunet-India M and Vázquez-Aguir J L 2008 Changes in North American extremes derived from daily weather data *J. Geophys. Res.* **113** D07113

Piao S, Mohammat A, Fang J, Cai Q and Feng J 2006 NDVI-based increase in growth of temperate grasslands and its responses to climate changes in China *Glob. Environ. Change* **16** 340–8

Posse G and Cingolani A M 2004 A test of the use of NDVI data to predict secondary productivity *Appl. Veg. Sci.* **7** 201–8

Potter C S and Brooks V 1998 Global analysis of empirical relations between annual climate and seasonality of NDVI *Int. J. Remote Sens.* **19** 2921–48

Rao C R N and Chen J 1995 Inter-satellite calibration linkages for the visible and nearinfrared channels of the advanced very high resolution radiometer on the NOAA-7, -9, and -11 spacecraft *Int. J. Remote Sens.* **16** 1931–42

Reich P B 1995 Phenology of tropical forest: patterns, causes, and consequences *Can. J. Bot.* **73** 164–74

Reynolds J F *et al* 2007 Global desertification: building a science for dryland development *Science* **316** 847–51

Richard Y, Martiny N, Fauchereau N, Reason C, Rouault M, Vigaud N and Tracol Y 2008 Interannual memory effects for spring NDVI in semi-arid South Africa *Geophys. Res. Lett.* **35** L13704

Schmidt H and Karnieli A 2000 Remote sensing of the seasonal variability of vegetation in a semi-arid environment *J. Arid Environ.* **45** 43–59

Schultz P A and Halpert M S 1993 Global correlation of temperature, NDVI and precipitation *Adv. Space Res.* **13** 277–80

Seager R *et al* 2007 Model projections of an imminent transition to a more arid climate in southwestern North America *Science* **316** 1181–4

Spano D, Cesaraccio C, Duce P and Snyder R L 1999 Phenological stages of natural species and their use as climate indicators *Int. J. Biometeor.* **42** 124–33

Srivastava S K, Jayaraman V, Rao P P N, Manikiam B and Chandrasekhar M G 1997 Interlinkages of NOAA/AVHRR derived integrated NDVI to seasonal precipitation and transpiration in dryland tropics *Int. J. Remote Sens.* **18** 2931–52

Tucker C J 1979 Red and photographic infrared linear combinations for monitoring vegetation *Remote Sens. Environ.* **8** 127–50

Tucker C J, Fung I Y, Keeling C D and Gammon R H 1986 Relationship between atmosphere CO$_2$ variations and a satellite-derived vegetation index *Nature* **319** 195–9

Tucker C J and Nicholson S E 1999 Variations in the size of the Sahara desert from 1980 to 1997 *Ambio* **28** 587–91

Tyson P O 1991 Climate change in southern Africa: past and present conditions and possible future scenarios *Clim. Change* **18** 241–58

van Mantgem P J *et al* 2009 Widespread increase of tree mortality rates in the western United States *Science* **323** 521–4

Walther G R, Post E, Convey P, Menzel A, Parmesan C, Beebee T J, Fromentin J M, Hoegh-Guldberg O and Bairlein F 2002 Ecological responses to recent climate change *Nature* **416** 389–96

Wang J, Rich P M and Price K P 2003 Temporal responses of NDVI to precipitation and temperature in the central Great Plains, USA *Int. J. Remote Sens.* **24** 2345–64

Zhang X, Friedl M A and Schaaf C B 2006 Global vegetation phenology from MODIS: evaluation of global patterns and comparison with in situ measurements *J. Geophys. Res.* **111** G04017

Zhang X, Friedl M A, Schaaf C B, Strahler A H and Liu Z 2005 Monitoring the response of vegetation phenology to precipitation in Africa by coupling MODIS and TRMM instruments *J. Geophys. Res. Atmos.* **110** D12103

Zhang X, Schaaf C B, Friedl M A, Strahler A H, Gao F, Hodges J F, Reed B C and Huete A 2003 Monitoring vegetation phenology using MODIS *Remote Sens. Environ.* **84** 471–5

Zhang X, Tarpley D and Sullivan J 2007 Diverse responses of vegetation phenology to a warming climate *Geophys. Res. Lett.* **34** L19405

Zhou L, Tucker C J, Kaufmann R K, Slayback D, Shabanov N V and Myneni R B 2001 Variation in northern vegetation activity inferred from satellite data of vegetation index during 1981 to 1999 *J. Geophys. Res.* **106** 20069–83